

## Study of the Drying Behavior of Poly(vinyl alcohol) Aqueous Solution

*Nadine Allanic, Patrick Salagnac,\* Patrick Glouannec*

Laboratoire d'Etudes Thermiques, Energétiques et Environnement, Centre de Recherche, BP 92116, 56 321 Lorient Cedex, France  
E-mail: patrick.salagnac@univ-ubs.fr

**Summary:** This paper deals with the drying behavior of poly(vinyl alcohol) aqueous solution containing an active substance and placed into a Petri box. The objective is to reduce the drying time while respecting some constraints. To succeed, it is important to understand complex mechanisms governing heat and mass transfers. During the drying, the product thickness shrinks and its properties evolve. Drying kinetics in convective and infrared radiation are presented.

**Keywords:** diffusion; drying; poly(vinyl alcohol); thermal properties

### Introduction

The aim of this work is to dry a polymer aqueous solution containing an active substance in a time compatible with an industrial production. Initially, the mixture with a 85% water volume fraction, is placed into a Petri box. The industrial drying process must be realised in a sterile atmosphere. As the proliferation of bacteria and the displacement of dust must be limited, convective drying with high air velocity is inadequate. Associating convective drying with infrared or microwave radiations is a solution frequently proposed in industrial process<sup>[1]</sup>. Indeed, the use of volatile organic solvents tends to be reduced and replaced by water. Due to the greater amount of energy necessary to evaporate water, mechanisms governing polymers drying have been investigated in lots of theoretical and experimental studies<sup>[2-4]</sup> to optimize energy requirement. Most of them have studied products with a low thickness. Lamaison<sup>[5]</sup> and Navarri<sup>[6]</sup> describe infrared drying, respectively of a painting and a PVA coating. Le Person<sup>[7]</sup> compares different drying modes (convection, conduction, infrared drying) of a thin pharmaceutical film. All these studies show that the direct energy supply appears to be an efficient solution. However, non-uniform radiant heating or high-intensity can damage polymer<sup>[8]</sup>.

In our study, a short infrared drying, associated with a low air flow is chosen. Several constraints must be respected. The Petri box temperature must be lower than 90°C (Petri box deformation stresses). The final product must be a thin film with a precise moisture

content and uniformly distributed at the bottom of the Petri box. During drying, the water evaporation from the surface creates concentration and temperature gradients. The thickness of polymer decreases, and its properties, including its microstructure, change considerably<sup>[9]</sup>.

In the first section, in order to understand heat and mass transfers, a physical model taking into account film shrinkage has been established. Then, thanks to experiments, the properties of the product are determined. Drying experimental curves in convection and infrared irradiation are presented. Finally, simulated and experimental results are compared for a convective drying.

## Heat and mass transfers model

During the drying process, the effect of evaporation is a one-dimensional shrinkage along the normal at the air-product interface. Figure 1 gives heat and mass transfers and boundary conditions applied to the Petri box and the mixture. Inside the product, transfers are supposed one dimensional (x-axis). Due to the great thickness, temperature gradients are not negligible. The thickness can be expressed as a linear function of the average moisture content  $\bar{X}$ <sup>[6,9]</sup>. Inside the product, mass transfer is liquid diffusion. The evaporation phenomena exists only on the air-product interface. The evaporation flux is given by<sup>[6]</sup>:

$$F_m = k_m \frac{M_v}{RT} (a_w P_{\text{vsat}} - P_{\text{va}}) \quad (1)$$

where  $k_m$  is the mass transfer coefficient,  $R$  the gaz constant,  $M_v$  the vapour molecular weight,  $P_{\text{vsat}}$  the saturated vapour pressure at surface of the mixture and  $P_{\text{va}}$  the air vapour pressure. Figure 2 gives activity  $a_w$  obtained by fitting experimental data by GAB model<sup>[10]</sup>. The curve has a similar profile to the Flory-Huggins model given for PVA by Perrin<sup>[11]</sup>. Activity is one of the key parameter of this study.

Thermal balance of the mixture and the conservation of the solvent are written as<sup>[5]</sup>:

$$\rho C_p \frac{\partial T}{\partial t} = \frac{\partial}{\partial x} \left( \lambda \frac{\partial T}{\partial x} \right) + \frac{\partial}{\partial x} \left( D_{AB} (C_{pA} \rho_A^0 - C_{pB} \rho_B^0) T \frac{\partial f_A}{\partial x} \right) + \phi \quad (2)$$

$$\frac{\partial f_A}{\partial t} = \frac{\partial}{\partial x} \left( D_{AB} \frac{\partial f_A}{\partial x} \right) \quad \text{with} \quad f_A = \frac{\rho^*}{\rho_A^0} \left( \frac{X}{1+X} \right) \quad (3)$$

where  $\rho$ ,  $C_p$  and  $\lambda$  are respectively the density, the specific heat and the thermal

conductivity of the mixture.  $D_{AB}$  is the diffusivity of water (A) diffusing through polymer (B) and  $f_A$  is the volume fraction. The infrared power, noted  $\phi$ , is given by the Lambert-Beer law<sup>[12]</sup> as a function of the extinction coefficient  $\kappa$  and  $\phi_0$  the infrared radiation at the polymer surface:

$$\phi = \phi_0 e^{-\kappa x} \quad (4)$$

For the Petri box, thermal balance takes into account heat conduction and infrared radiation source term. The product and the Petri box are semi-transparent media. Hence, power must be correctly chosen in order to avoid skin formation at polymer surface and deformation of the Petri box.

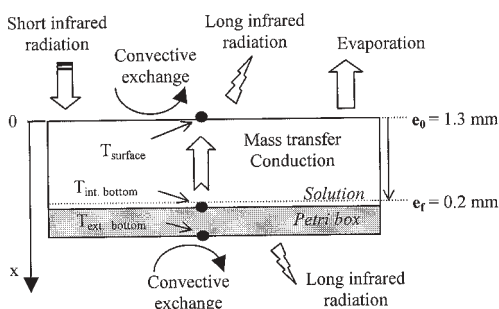


Figure 1. Heat and mass exchanges.

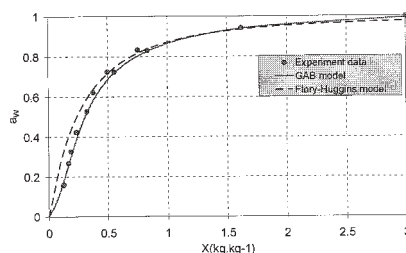


Figure 2. Activity.

## Results and discussions

### Materials and experiments

The drying equipment, which has been described previously<sup>[13]</sup>, enables us to combine convective and infrared drying. The infrared emitter, working in the short infrared range, is placed on the upper side of the chamber. Temperatures inside and outside the Petri box are measured by two thermocouples with a  $75\mu\text{m}$  diameter (cf. Figure 1). An optical pyrometer gives the surface temperature of the polymer. An electronic scale is used to acquire the product mass as a function of time. Final products will be dry under a laminar flow in a sterile atmosphere. To have similar conditions to the industrial process, the air enters in the drying chamber with a low velocity ( $v = 0.5 \text{ m.s}^{-1}$ ) and a low relative humidity ( $H_r = 20 \%$ ).

### ***Mixture diffusivity and infrared absorptivity determination***

For low moisture content, diffusion is the main phenomena and determines drying kinetics. Therefore, diffusion coefficient is an important parameter to estimate. Usually, it is identified thanks to drying curves by inverse method<sup>[14]</sup>. An exponential dependence of the diffusion coefficient on the solvent content and temperature is proposed in literature for lots of polymer solutions<sup>[6,11,15]</sup>. The following expression has been chosen:

$$D_{AB} = D_0 e^{\frac{E_{ad}}{RT}} e^{\frac{a}{X}} \quad (5)$$

The values of activation energy  $E_{ad}$  and coefficient  $a$  are the ones found by Navarri<sup>[6]</sup> for poly(vinyl alcohol) ( $E_{ad} = 31700 \text{ J.mol}^{-1}$  and  $a = 0.332$ ). In the case of constant diffusion coefficient and thickness, the Fick's second law has an analytical solution<sup>[15]</sup>. It allows to identify the initial diffusivity thanks to convective drying kinetics. Then, we deduce from this value, the coefficient  $D_0 = 5.27 \cdot 10^{-6} \text{ m}^2.\text{s}^{-1}$ .

In infrared drying, the evaporation rate and the temperature evolution depend on spectral distribution of the irradiation and radiative properties of the product. Figure 3 presents the polymer solution transmissivity ( $\tau$ ) for a thickness of 1.3 mm. These measures are obtained with a FTIR spectroscopy and compared with water spectrum<sup>[16]</sup>. The dimensionless spectral infrared irradiation is also presented. Therefore, the emitters are identified as a black body with an emissive temperature of  $2000 \text{ K}$ <sup>[12]</sup>. During drying, the equivalent transmittivity of the mixture is expressed as a function of the average water volume fraction and the thickness ( $e$ ):

$$\tau = \tau_A \tau_B = e^{-\kappa_A \bar{f}_A e} e^{-\kappa_B (1-\bar{f}_A) e} \quad (6)$$

where  $\tau_A$ ,  $\tau_B$  and  $\kappa_A$ ,  $\kappa_B$  are respectively the equivalent transmissivity and the total absorptivity of the water and the polymer. Thanks to latter curves, we can determinate  $\kappa_A = 555 \text{ m}^{-1}$  and  $\kappa_B = 2300 \text{ m}^{-1}$  and deduce equivalent transmittivity during drying. On the other hand, the equivalent transmissivity has been determined by measuring the total flux received by the product (Petri box + mixture) and transmitted. These measures were made with a sensor developed in the laboratory<sup>[17]</sup>. First, the total absorptivity of the Petri box was determinated ( $\kappa_{\text{box}} = 265 \text{ m}^{-1}$ ). Figure 4 demonstrates that it exists a good agreement between the two methods. A small difference appears for low moisture content, maybe because we don't take into account reflexion at different interfaces. During drying, due to water evaporation, the product transmittivity varies. Changes in composition and a decreasing of the thickness involve a decreasing of absorptivity. At the end of the drying,

the mixture absorbs only 15 % infrared irradiation. It is less than the irradiation absorbed by the Petri box.

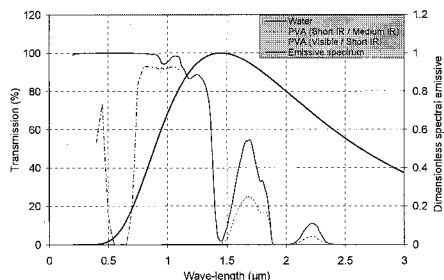


Figure 3. Transmissivity of water and PVA. and dimensionless spectral emissive power.

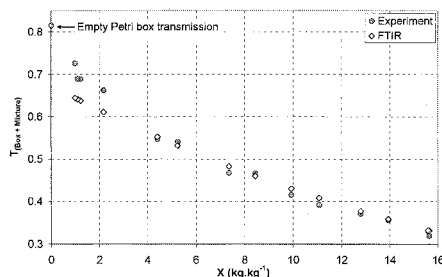


Figure 4. Evolution of the equivalent Transmissivity.

### Drying kinetics analysis

The influence of infrared intensity on drying time and quality is now analyzed. Figure 5 gives variation of the evaporation rate as a function of moisture content for different initial values of the infrared intensity and for a time horizon of five minutes. Increasing infrared intensity enables us obtain a higher evaporation rate. However, the first drying stage (activity close to one) is smaller. The solvent concentration at the surface falls down quicker involving important decreasing of the evaporation rate and of the diffusion term. At this time, drying is no more controlled by evaporation, but limited by diffusion phenomena. Moreover, during this stage, surface temperature increases all the more so since infrared intensity is higher<sup>[6,18]</sup>. The polymer and the Petri box can be damaged, that is the reason why it is important to regulate energy inputs. In this aim, a model is developed, based on heat and mass equations previously presented (1-4). These are solved by control volume method with implicit scheme (number of control volumes: 50, time step: 0.2 s). Figure 6 presents experimental and simulated results for a convective drying. Until 6000 s, a good agreement is observed between simulated and experimental curves. After this time, diffusivity is certainly surrounding, involving higher temperatures than experimental ones. The experimental evaporation rate decreasing is also not important enough, maybe because of skin formation at the surface or changes in microstructure<sup>[17]</sup>. This test shows that it is necessary to estimate a better diffusion coefficient using inverse methods before trying to simulate infrared drying kinetics.

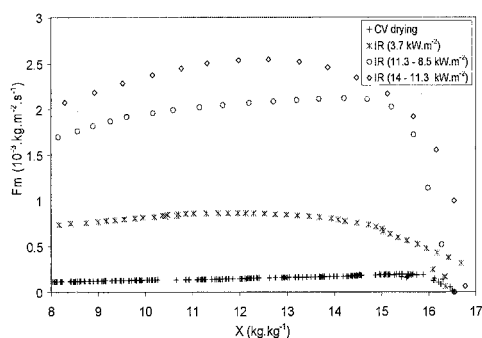


Figure 5. Evaporation rate evolution vs moisture content for different initial powers.

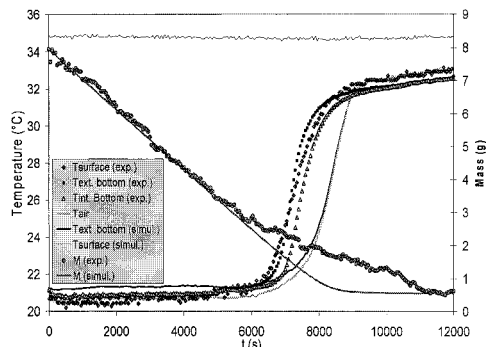


Figure 6. Convective drying kinetics.

## Conclusion

In this study, mechanisms limiting drying of poly(vinyl alcohol) have been analyzed. Absorptivity and diffusivity, which are key parameters of this problem, are estimated as a function of moisture content and of other parameters (temperature, thickness,...). Experimental drying kinetics have shown the importance of the energy input adapted to the mixture and Petri box thermal behavior. To optimize drying time, it is necessary to anticipate skin formation and to find a way to delay it.

- [1] Jonkers G., Nienhuis J.G., Van De Velde B., *Macromolecular Symposium*, **2002**, 187, 249-260.
- [2] Ventras J.S., Ventras M., *Journal of Polymer Science, Part B : Polymer physics*, **1994**, 32, 187-194.
- [3] Yoshida M., Miyashita H., *Chemical engineering Journal*, **2002**, 86, 193-198.
- [4] Carra S., Pinoci D., Carra S., *Macromolecular Symposium*, **2002**, 187, 585-596.
- [5] Lamaison V., Scudeller Y. & al., *International Journal of Thermal Science*, **2001**, 40, 181-194.
- [6] Navarri P., Andrieu J., *Chemical Engineering and Processing*, **1993**, 32, 319-325.
- [7] Le Person S., Puiggali J.R. & al., *Chemical Engineering and Processing*, **1998**, 37, 257-263.
- [8] Chen J.J., Lin J.D., *International Journal of Heat and Mass Transfer*, **2000**, 43, 2155-2175.
- [9] Guerrier B., Bouchard C., Allain C., Bénard C., *AIChE Journal*, **1998**, 44, 4, 791-798.
- [10] Srinivasa P.C., Ramesh M.N. & al., *Carbohydrate Polymers*, **2003**, 53, 431-438.
- [11] Perrin L., Nguyen Q.T., Clement R., Noel J., *Polymer International*, **1996**, 39, 251-260.
- [12] Incropera F.P., De Witt D. P., *Fundamentals of heat and mass transfer*, 5th ed., Eds. Wiley & Sons, New York 2002.
- [13] Glouannec P., Lecharpentier D., Noel H., *Applied Thermal Engineering*, **2002**, 22, 1689-1703.
- [14] Doumenc F., Guerrier B., *AIChE Journal*, **2001**, 47, 5, 984-993.
- [15] Ion L., Vergnaud J.M., *Polymer Testing*, **1995**, 14, 479-487.
- [16] Hale G. M., Query M. R., *Applied Optical*, **1973**, 12, 555-563.
- [17] Noël H., Ploteau J.P., Glouannec P., *Proceedings, 8<sup>th</sup> International Symposium on Temperature and Thermal Measurements in Industry Science*, **2001**, 925-930.
- [18] Yoshida M., Miyashita H., *Chemical Engineering Journal*, **2002**, 86, 193-198.